Title	Magnetic properties of microwave-plasma (thermal) chemical vapour deposited Co-filled (Fe-filled) multiwall carbon nanotubes: comparative study for magnetic device applications
Authors	Mathur, A.;Maity, Tuhin;Wadhwa, Shikha;Ghosh, B.;Sarma, Sweety;Ray, Sekhar C.;Kaviraj, Bhaskar;Roy, Susanta S.;Roy, Saibal
Publication date	2018-07-04
Original Citation	Mathur, A., Maity, T., Wadhwa, S., Ghosh, B., Sarma, S., Ray, S. C., Kaviraj, B., Roy, S. S. and Roy, S. (2018) 'Magnetic properties of microwave-plasma (thermal) chemical vapour deposited Co-filled (Fe-filled) multiwall carbon nanotubes: comparative study for magnetic device applications', Materials Research Express, 5(7), 076101 (8pp). doi: 10.1088/2053-1591/aacddb
Type of publication	Article (peer-reviewed)
Link to publisher's version	10.1088/2053-1591/aacddb
Rights	© 2018, IOP Publishing Ltd. This is an author-created, un-copyedited version of an article accepted for publication in Materials Research Express. The publisher is not responsible for any errors or omissions in this version of the manuscript or any version derived from it. The Version of Record is available online at: https://iopscience.iop.org/article/10.1088/2053-1591 - https://creativecommons.org/licenses/by-nc-nd/3.0/
Download date	2024-04-19 08:23:36
Item downloaded from	https://hdl.handle.net/10468/11797

University College Cork, Ireland
Coláiste na hOllscoile Corcaigh

Materials Research Express

Magnetic properties of microwave-plasma (thermal) chemical vapour deposited co-filled (Fe-filled) multiwall carbon nanotubes: Comparative study for magnetic device applications

To cite this article before publication: Ashish mathur *et al* 2018 *Mater. Res. Express* in press https://doi.org/10.1088/2053-1591/aacddb

Magnetic Properties of Microwave-Plasma (Thermal) Chemical Vapour deposited *Co-filled* (*Fe-filled*) Multiwall Carbon Nanotubes: Comparative Study for Magnetic Device Applications

A. Mathur[a], Tuhin Maity[b,Ψ], Shikha Wadhwa[a], B. Ghosh[c], Sweety Sarma[c], Sekhar C. Ray[c,*], Bhaskar Kaviraj[d], Susata S. Roy[d] and Saibal Roy[b,e]

[a] Amity Institute of Nanotechnology, Amity University Uttar Pradesh, Noida 201301, India.

[b] Tyndall National Institute, Cork, Ireland.

[c] Department of Physics, CSET, University of South Africa, Private Bag X6, Florida, 1710, Science Campus, Christiaan de Wet and Pioneer Avenue, Florida Park, Johannesburg, South Africa.

[d] Department of Physics, School of Natural Sciences, Shiv Nadar University, Gautam Budh Nagar 201314, Uttar Pradesh, India.

[e] Department of Physics, University College Cork (UCC), Cork, Ireland.

Abstract: "*Co-filled*" and "*Fe-filled*" multiwall carbon nanotubes (MWCNTs) were grown using microwave-plasma chemical vapour deposition (MPCVD) and thermal chemical vapour deposition (TCVD) methods respectively, and their structural and magnetic properties were studied for magnetic device applications. Scanning electron microscopy (SEM) and transmission electron microscopy (TEM) images show that the average tube length ≈ 80-500 μm with outer (inner) diameter ≈ 20-50 (≈ 10-20) nm for MWCNTs prepared by both methods. The diffraction peaks of both x-ray diffraction pattern show that the interlayer distance, d_{002} ≈ 3.36Å, which is comparable to the graphite structure (d_{002} = 3.35Å). The graphitic crystallite sizes (L_a) of MPCVD (TCVD) synthesized MWCNTs are ≈ 24.78 nm (≈ 22.13 nm) as obtained from the intensity ratio of (I_D/I_G) D-peak, the disordered structure of graphite and G-peak, the C-C bond in graphitic structure of Raman spectra. The magnetization of "*Fe-filled*" TCVD grown MWCNTs is much higher than "*Co-filled*" MPCVD grown MWCNTs due to the formation of higher content of Fe-C and/or Fe-oxides in the MWCNT structures. The higher magnetic coercivity ≈ 2900 Oe and formation of isolated single-domain Fe-nanoparticles in "*Fe-filled*" TCVD grown MWCNTs, as found from SEM / TEM micrographs, makes the ferromagnetic MWCNTs as a promising material for the high-density magnetic recording media.

* Corresponding Author: Sekhar C. Ray (Raysc@unisa.ac.za)

Ψ Present address: Department of Materials Science, University of Cambridge, Cambridge, UK.

1. Introduction

Study of the magnetic recording on a hard disk reveals that none of the critical dimensions exceed one micron: bit length, track width, media thickness and read head size are all measured in nanometres. An effect called ballistic magnetoresistance has been demonstrated to have the capability of producing read heads that can deal with storage densities of 1Tb/in².– 10x, which is the density expected in the next generation of hard drives. Commercial application of spintronic in electronics is farther away but the promise is there! The carbon nanotubes (CNTs) is one of the materials that became a worldwide research focus only after fullerenes were discovered and after single-walled carbon nanotubes (SWNTs) were introduced to the research community in 1993 [1]. These CNTs are classified into SWCNTs, double walled carbon nanotubes (DWCNTs) and multi-walled carbon nanotubes (MWCNTs) with regard to the number of graphene layers constituting their wall. Due to simplicity of their synthesis with / without metal-catalyst and the diversity of their properties [2], CNTs quickly propelled into electronics, optics, nano- and biotechnology research labs around the world. Particularly, metal-catalyst like Fe, Co and Ni based ferromagnetic-CNT materials have potential applications in various areas such as “magnetic storage media” that include the traditional tapes and video-cassettes, hard disks for mainframe computers, floppy disks for personal computers (PC), portable ZIP and MO disks (magneto-optic) with high storage capacity [3-5]. For storage capacity, a minimum signal spot of < 100 nm is required for a terabyte capacity and < 20 nm for greater than terabyte capacity. The “magnetic storage media” can be broadly divided into two categories; i.e. the horizontally oriented and vertically oriented types. These results indicate that the horizontally oriented magnetic storage media may reach the physical limit for the storage capacity of >40 Gbit/in.^{2} [6, 7]. In the present commercial market, a few hard-disk manufacturers and research institutes have successfully designed such prototype media to demonstrate their feasibility [6, 8-10].

For the fabrication of these devices, high precision design, and cost effective fabrication techniques are of utmost importance. In addition, the fabrication parameters such as size uniformity, morphology and control of magnetic properties such as higher coercive field strength H_c, higher squareness ratio S, higher anisotropic magnetic crystal and lower noises are also needed to take into account for the fabrication of

these devices. Based on these material properties for the fabrication of magnetic storage media using MWCNTs, we report in the present work about the magnetic properties of "*Co-filled*" and "*Fe-filled*" MWCNTs grown by MPCVD (TCVD) process and hence studied/compared their structural and magnetic behaviours for possible potential applications in the high-density magnetic memory data storage media.

2. Experimental details

We have grown MWCNTs on silicon substrate by the two different process *viz.* MPCVD and TCVD. In MPCVD process, the MWCNTs are grown on DC-sputtered "*Co-deposited"* (≈ 3 nm) un-oxidised *p*-type, <100> silicon substrate by the mixture of N_2 and CH_4. Prior to growing MWCNT in the MPCVD process, the "*Co-deposited*" (~ 3 nm) silicon substrate were pre-treated at ~ 750°C using microwave-power of 300 W, for ~ 2 min in nitrogen plasma atmosphere. The nitrogen plasma pre-treatment on the "*Co-deposited*" silicon substrate breaks the Co-thin-film into nanoparticles that act as catalytic sites for the growth of MWCNTs. After the pre-heat-treatment, microwave power was increased immediately up to ~ 600 W. During the MWCNTs growth phase the CH_4 provides carbon for nanotube growth, whereas the N_2 etches the amorphous carbon (a-C) by-products from the deposition process, greatly reducing the amount of a-C deposited with the CNTs. In the TCVD process, the MWCNTs is grown on *p*-type, <100> silicon substrate at ~750°C temperature in oxygen plasma atmosphere. In TCVD, process a requisites mixture of ferrocene, the source of "*Fe-catalyst*" and toluene, the source of carbon are used as a precursor. Ferrocene is used for the "*Fe-catalyst*" and to thermally dissociate the toluene molecule to form the MWCNTs. Details of different growth phases of TCVD and MPCVD process are available elsewhere [11]. The CNTs morphology and microscopic details of the structure are determined by the scanning electron microscopy (SEM, FEI 3D Quanta) and high-resolution transmission electron microscopy (TEM, JEOL2010) at an accelerating voltage of 120 kV. The wide-angle region of the X-ray diffraction (XRD) patterns is used to determine the lattice structure using Rigaku D/max-2400 diffractometer with a Cu K_α wavelength X-ray source. Raman spectra were measured using an Ar^+ laser of excitation wavelength ~ 514.5 nm (E_{ex} = 2.41 eV) with a spot size of approximately 2-3 mm, yielding a spectral resolution of better than 2 cm^{-1}. Due care was taken to minimize

heating of MWCNTs by using a low laser power of < 2 mW to minimize desorption and/or oxidation by the laser-induced heating of de-oxidized MWCNTs. A SQUID type magnetometer (MPMS, Quantum Design) with a sensitivity of $< 5\times 10^{-8}$ emu, was used to measure the magnetisation M-H loops for the TCVD and MPCVD grown MWCNTs as a function of applied magnetic field in the range -5 T< H < +5T and at the temperatures of 2 K, 150 K and 300 K respectively. The dimension of MPCVD / TCVD grown MWCNTs kept same for this measurement as well as comparisons of magnetization. The temperature dependent field-cool (FC) and zero field cool (ZFC) magnetization measurements were carried out within the temperature range 2 K - 350 K at a constant magnetic field of 20 Oe. During the temperature-dependent FC / ZFC magnetization measurements the MWCNTs were cooled-down first from room temperature 300 K to 2 K with cooling rate of 10 K/min. After that, a very low magnetic field ~ 20 Oe is applied and the magnetization is measured as a function of temperature with heating temperature step ~ 2.5 K at a rate of 10 K/min.

3. Results and Discussion

The general morphology of SEM and TEM images of MPCVD (TCVD) grown MWCNTs are shown in Fig. 1. As can be seen in the upper panel of Fig. 1(a) & 1(b), the cross-sectional and 45^0 tilted (inset) SEM images of MWCNT forests show the formation of well-aligned vertical tubular structure of MWCNTs. The MPCVD-grown MWCNTs (upper panel of Fig 1a) are less dense than TCVD-grown MWCNTs (upper panel of Fig 1b) and their estimated lengths are ~ 20 μm, and ~ 300 μm for MPCVD and TCVD grown MWCNTs, respectively, which implies that the growth rate of MWCNTs is higher in TCVD process. The SEM images of TCVD-grown tubular structured MWCNTs show a significant amount of bright material on the top surface, associated with amorphous carbon and, probably, residual "*Fe-catalyst*". It can also be observed that the content of "*Fe-catalyst*" is higher in TCVD grown MWCNTs than the presence of "*Co-catalyst*" in MPCVD grown MWCNTs. Lower panel of Fig. 1(a) & 1(b) shows the high resolution-TEM images, which confirms the formation of tubular structure with the presence of "*Co-catalyst*" ("*Fe-catalyst*") MPCVD (TCVD) grown MWCNTs. The high-resolution TEM images confirm that the tubes are multi-

walled in nature, with black spot metal-catalyst visible in the nanotube cores that may influence the overall magnetic properties of MWCNTs [12]. The outer and inner diameters of both MWCNTs are estimated from the high-resolution TEM and that are ≈ 20-50 nm and ≈ 10-20 nm respectively.

Fig. 2(a) shows the X-Ray diffraction patterns of both MWCNTs. Different graphitic reflection planes along with metallic carbide/oxides are identified/indexed in the spectra. The diffraction peaks at $2\theta \approx 26^0$ (002) and $2\theta \approx 53^0$ (004) are associated with the interlayer spacing between the graphene planes. A peak at $2\theta \approx 43^0$ (100) is the characteristic of two-dimensional in-plane symmetry along the graphene layers. The position and width of the (002) peak is related to the structural ordering of the material. The $d_{002} \approx 3.36$ Å diffraction peak is derived from the most prominent (002) reflection of graphite peak around $2\theta \approx 26^0$ and comparable with pure graphite ($d_{002} = 3.35$Å). However, the (002) peak of the TCVD grown MWCNTs is broader at the base that may indicate a two-phase crystalline system, or a slight increase in the *d* spacing between the walls in a relatively small number of tubes. The XRD patterns of TCVD MWCNTs show some other peaks and are ascribed to the formation of Fe/Fe_3C/Fe-oxides in accordance with earlier reports [13, 14]. MPCVD MWCNTs also show a few peaks apart from C and are assigned as Co/Co_3C [15, 16]. For BCC α-Fe, the accepted critical size for the single domain particle is about ~ 20 nm [12]. We have therefore assumed that the TCVD grown MWCNTs have *Fe-particles* that are single domain, thus enhancing the magnetic behavior in them. Raman spectra of MPCVD and TCVD grown MWCNTs are shown in Fig. 2(b). The Raman spectra of all crystalline graphitic material exhibits four bands, denoted as D, G, D′ and 2D. The G band corresponds to the tangential stretching (E_{2g}) mode of highly oriented pyrolytic graphite. The origin of the disorder-induced D and D′ band and 2D, overtone of D band, is observed in our crystalline graphitic MWCNTs [17-19]. The presence of the D and D′ bands indicate defects in the crystallite structure and edges of MWCNTs. The G band of MPCVD (TCVD) grown MWCNTs at 1575 cm^{-1} (1573 cm^{-1}) is assigned to the in-plane vibration of the C–C bond with a shoulder around 1616 cm^{-1} (1618 cm^{-1}), typical defective graphite-like materials and the band at 1345 cm^{-1} (1348 cm^{-1}) activated by the presence of disorder in carbon systems (D band). The Raman spectra of MPCVD (TCVD) grown MWCNTs also show a band at 2691 cm^{-1} (2686 cm^{-1}) denoted as 2D band, which is attributed to the overtone of the D band. All the Raman

bands, I_D/I_G ratios and in-plane graphite crystallites sizes (La) are obtained after deconvolution of Raman spectra using best Gaussian functions fittings as shown in fig. 2(c) & 2(d) for MPCVD and TCVD grown MWCNTs respectively. G and 2D band in the Raman spectra of MPCVD grown MWCNTs are shifted to higher wavenumbers as compared to TCVD grown MWCNTs indicating a less inter-tube interactions. The I_D/I_G ratio of TCVD grown MWCNTs is higher (~ 0.75) than MPCVD grown MWCNTs (~ 0.67), as obtained from the integrated intensity ratio of D-band and G-band, that further indicates the TCVD grown MWCNTs have more defects, higher disorder and higher graphitic in nature. However, we have estimated the in-plane graphite crystallites sizes (La) of these MWCNTs using the relation [20, 21]: La (nm) = $(560/E_L^4).(I_D/I_G)^{-1}$; where E_L is the laser excitation energy (E_{ex} = 2.41 eV). We found that the TCVD grown MWCNTs have smaller crystallites sizes (≈ 22.12 nm) than MPCVD grown MWCNTs (≈ 24.78 nm). All the parameters obtained from Raman spectra are given in Table I.

The magnetic hysteresis (M-H) loops and temperature dependent field-cool (FC) and zero field cool (ZFC) magnetization (M-T) of MPCVD (TCVD) grown MWCNTs are shown in Fig. 3 (Fig. 4). The magnetic hysteresis M-H loops are measured within the applied magnetic field range of -5T to +5T at three different temperature 300 K, 150 K and 2 K respectively. The FC and ZFC (M-T) curves are measured at a constant magnetic field of ~ 20 Oe. The TCVD grown MWCNTs showing symmetric magnetic hysteresis (M-H) loops (Fig. 4a) exhibits a clear ferromagnetic behavior as compared to MPCVD grown MWCNTs (Fig. 3a). The room temperature saturation magnetic moment (Ms) and remanence magnetic moment (Mr) of the MPCVD grown "*Co-filled*" MWCNTs is nearly 6-7 times lower than TCVD grown "*Fe-filled*" MWCNTs. The magnetization of MPCVD grown MWCNTs gradually decreases above H > 10000 Oe, which results from the diamagnetic contribution. Moreover, we strongly believe that the disappearance of ferromagnetic behavior is either due to the formation of Co-carbides and/or Co-oxides with specific composition or the increase of kinetic bandwidth. In case of TCVD grown MWCNTs, the saturation magnetization field is lower than 10000 Oe, indicating the better magnetization than MPCVD grown MWCNTs. The room temperature magnetic coercivity (Hc) of TCVD grown "*Fe-filled*" MWCNTs is 12-13 times higher (~ 500 Oe, Fig. 4b) than that of MPCVD grown "*Co-filled*" MWCNTs (~ 40 Oe, Fig. 3b) and bulk counterpart Fe /

Co ($Fe_{Bulk} \approx 0.9$ Oe and $Co_{Bulk} \approx 10$ Oe) [22-24] metals, that are comparable to the values obtained elsewhere [8,9]. We have extracted the different magnetic parameters of MPCVD and TCVD grown MWCNTs from the M-H loops in Figures 3(a-b) and 4(a-b) respectively and that are given in Table I; where we find that the magnitudes of Ms, Mr and Hc are gradually increasing with decrease of temperature (300 K→2K). However, these findings are encouraging for various technological applications and suggest the higher magnetic stability. Another character of the magnetization parameter is the remanent magnetization ratio, Mr/Ms (ratio of the remanent magnetization over the saturation magnetization). According to the Stoner-Wohlfarth model [25], in a randomly oriented single-domain particle system, the Mr/Ms ratio should be 0.5, which is exactly the situation observe below the room temperature in our TCVD grown MWCNTs as shown in Fig. 4(a-b) and Table I. For single-domain particle with a uniaxial anisotropy and randomly distributed easy axes, the ratio of Mr/Ms ≈ 0.5 at a temperature well below the blocking temperature. Therefore, an increase in both Mr/Ms and H_C with decreasing temperature can be explained by depinning of domain walls in the particles. In TCVD grown MWCNTs, the "Fe" particles used as the seeds for the nucleation are small enough (< 20 nm) and the particles are single domain and exhibit very high uniaxial anisotropy due to the stress and shapes of MWCNTs [26]. Consequently, the coercive field was enhanced significantly (2900 Oe at 2K) that satisfy the requirement of Hc ≈ 2.5 kOe for the next generation high-density recording media [27]. Furthermore, the "Fe"- particles being inside the tube make the walls of the nanotubes as a non-magnetic separators, a quality which is essential for high-density magnetic recording media in order to eliminate the dipolar interaction between the neighboring particles [23]. Fig. 3(c) and 4(c) show the field-cool (FC) and zero field cool (ZFC) magnetization curves in the temperature range of 2 K to 350 K recorded at 20 Oe external applied magnetic field. For ZFC curve, the MWCNTs was cooled down to 2 K in absence of magnetic field and the magnetization (M_{ZFC}) was recorded during the increase of temperature by applying a magnetic field of 20 Oe, whereas for FC measurement, the MWCNTs was cooled down to 5 K at 20 Oe, and the magnetization (M_{FC}) was recorded while increasing the temperature. It is observed that FC and ZFC curves are bifurcated ~ 220 K in MPCVD grown MWCNTs (Fig. 3c), which is attributed to the transition from relaxation to blocked state of the nano-particles of very low dimension

embedded inside the nanotubes that behave like superparamagnetic (SPM) particles due to single domain configuration [28]. This temperature is defined as blocking temperature (T_B) and this nature of FC-ZFC curve represents the SPM relaxation. The maximum value of magnetic moment obtained by ZFC plot is different from T_B and is denoted as T_P. The value of T_P in FC-ZFC magnetization curves in MPCVD grown MWCNTs was 45 K. This difference between T_B and T_P indicates the particles distribution within the system and due to the smaller particles, the ZFC curve just starts to decrease below ~ T_P. However, the FC-ZFC curves coincide at the highest measured temperature at 350 K in TPCVD grown MWCNTs as shown in Fig. 4(c). Thus, the blocking temperature in this system is close to this value. The increase of ZFC magnetization with temperature indicates a dipolar coupling between the particles, whereas a near flat FC curve indicates a strong demagnetizing effect [29]. The observed decrease of low field ZFC and the increase of irreversibility with decreasing temperature from 350 K can be attributed to the passage from a ferromagnetic state to a low temperature disordered surface regime that consistence with the remnant (M_{REM}) curved of TCVD grown MWCNTs obtained from the FC and ZFC curve ($M_{REM} = M_{FC} - M_{ZFC}$). Local anisotropy at the grain surface increases more sharply than the exchange interaction parameter due to lack of symmetry at grain surface. The difference between the M_{FC} and M_{ZFC} provides the information about the nature of blocking temperature as well as the magneto crystalline anisotropy of the nanoparticles [28]. The magnetic anisotropy constant determined from the differences between the ZFC and FC magnetizations were significantly higher in TPCVD grown MWCNTs than MPCVD grown MWCNTs and that are probably due to the different particle size distribution in the system as a result higher magnetic properties were obtained in TPCVD grown MWCNTs.

4. Conclusion

We have grown the *Co-filled* (*Fe-filled*) MWCNTs on Si-substrate by the MPCVD (TCVD) process and found that the TCVD grown MWCNTs are denser and longer than the MPCVD grown MWCNTs with an average inner tube diameter ≈ 10-20 nm. Different Raman bands of TCVD grown MWCNTs occurred at lower wave numbers (cm^{-1}) than MPCVD grown MWCNTs, due to less stress and higher amorphous carbon

content present in the TCVD-grown MWCNTs structure. The Raman results also suggest the presence of higher defect levels in the TCVD-grown MWCNTs. The magnetic properties of TCVD grown MWCNTs are enhanced and comparable with bulk-Co/Fe metals. The magnetic parameters Ms, Mr and Hc are 7, 70 and 35 times higher in TCVD grown MWCNTs than MPCVD grown MWCNTs. The magnetic behaviour of MWCNTs are enhanced with the decrease in temperature. The decrease of low field ZFC and the increase of irreversibility with decreasing temperature from 350 K $\rightarrow$ 2K, can be attributed to the passage from a ferromagnetic state to a low temperature disordered surface regime. These ferromagnetic MWCNTs are ideal building blocks for future bonded, consolidated as well as thin film magnets with high energy density and high thermal stability. Considering TCVD grown MWCNT's cost-effective production and high coercive field $\approx$ 2.9 kOe satisfying the requirement of Hc $\approx$ 2.5 kOe, it can be considered as a promising material for the next generation high-density recording media.

Acknowledgments

This work was supported by National access programme (NAP) from Tyndall National institute, Cork, Ireland (Grant no. NAP-613). S.C.R. and S.S. gratefully acknowledge the financial support received from the NRF, South Africa (Grant No. EQP13091742446 and 99677). B.G. wishes to acknowledge the financial support of the VR-CSET program in the University of South Africa.

References

[1] Iijima S and Ichihashi T 1993 Single-shell carbon nanotubes of 1-nm diameter *Nature* **363** 603

[2] Saito R, Dresselhaus G and Dresselhaus M S 1998 Physical properties of carbon nanotubes *Imperial College Press* London

[3] Chou S Y, Wei M S, Kraus P R and Fisher P B 1994 Single-domain magnetic pillar array of 35 nm diameter and 65 Gbits/in.^{2} density for ultrahigh density quantum magnetic storage *J. Appl. Phys.* **76** 6673

[4] Li D C, Dai L, Huang S, Mau A W H and Wang Z L 2000 Structure and growth of aligned carbon nanotube films by pyrolysis *Chemical Physics Letters* **316** 349

[5] Geng J, Jefferson D A and Johnson B F G 2004 Direct conversion of iron stearate into magnetic Fe and Fe_3C nanocrystals encapsulated in polyhedral graphite cages Chem. *Commun.* **0** 2442

[6] Todorovic M, Schultz S, Wong J and Scherer A 1999 Writing and reading of single magnetic domain per bit perpendicular patterned media *Appl. Phys. Lett*. **74** 2516

[7] Speliotis D E 1999 Magnetic recording beyond the first 100 Years *J. Magn. Magn*. Mater. **193** 29

[8] Kuo C T, Lin C H and Lo A Y 2003 Feasibility studies of magnetic particle-embedded carbon nanotubes for perpendicular recording media *Diamond Relat. Mater*. **12** 799

[9] Geng F and Cong H 2006 Fe-filled carbon nanotube array with high coercivity *Physica B:Condens. Matter.* **382** 300

[10] Zhang X X, Wen G H, Huang S M, Dai L M, Gao R P, Wang, Z L 2001 Magnetic properties of Fe nanoparticles trapped at the tips of the aligned carbon nanotubes *J. Magn. Magn. Mater.* **231** 9

[11] Mathur A, Wadhwa S, Tweedie M, Hazra K S, Dickinson C, Roy S S, Mitra S K, Misra D S and McLaughlin J A 2011 A comparative study of the growth, microstructural and electrical properties of multiwall CNTs grown by thermal and microwave plasma enhanced CVD methods *Physica E* **44** 29

[12] Zilli D, Chiliotte C, Escobar M M, Bekeris V, Rubiolo G R, Cukierman A L and Goyanes S 2005 Magnetic properties of multi-walled carbon nanotube-epoxy composites *Polymer* **46** 6090

[13] Liu S and Wehmschulte R J 2005 A novel hybrid of carbon nanotubes/iron nanoparticles: iron-filled nodule-containing carbon nanotubes *Carbon* **43** 1550

[14] Emmenegger C, Bonard J M, Mauron P, Sudan P, Lepora A, Grobety B, Zuttel A and Schlapbach L 2003 Synthesis of carbon nanotubes over Fe catalyst on aluminium and suggested growth mechanism *Carbon* **41** 539

[15] McHenry M E, Majetich S A, Artman J O. DeGraef M and Staley S W 1994 Superparamagnetism in carbon-coated Co particles produced by the Kratschmer carbon arc process *Phys. Rev. B* **49** 11358

[16] Mishra A, Jain G and Ninama S 2014 Surface morphology and X-ray diffraction studies of Co (II) complexes of pyrazole ligands *Journal of Physics: Conference Series* **534** 012034

[17] Tuinstra F and Koenig J L 1970 Raman Spectrum of Graphite *J. Chem. Phys.* **53** 1126

[18] Wilhelm H, Lelaurain M, McRae E and Humbert B 1998 Raman spectroscopic studies on well-defined carbonaceous materials of strong two-dimensional character *J. Appl. Phys.* **84** 6552

[19] Dresselhaus M S, Pimenta M A and Eklund P C, Dresselhaus G, Weber W H and Merlin R (Eds.) 2000 *Raman Scattering in Material Science*, Springer, Berlin

[20] Cançado L G, Takai K, Enoki T, Endo M, Kim Y A, Mizusaki H, Jorio A, Coelho L N, Magalhães-Paniago R and Pimenta M A 2006 General equation for the determination of the crystallite size La of nanographite by Raman spectroscopy *Appl. Phys. Lett.* **88** 163106

[21] Soin N, Roy S S, Ray S C and McLaughlin J A 2010 Excitation energy dependence of Raman bands in multiwall carbon nanotubes *J. Raman Spectroscopy* **41** 1227

[22] Bozorth R M 1951 Ferromagnetism *D. Van Nostrand Company Inc*., New York

[23] Whitney T M, Jiang J S, Searson P C, and Chien C L 1993 Fabrication and magnetic properties of arrays of metallic nanowires *Science* **261** 1316

[24] Luo H, Wang D, He J and Lu Y 2005 Magnetic Cobalt Nanowire Thin Films *J. Phys. Chem. B* **109** 1919

[25] Stoner E C and Wohlfarth E P 1948 A mechanism of magnetic hysteresis in heterogeneous alloys *Phil. Tran. Roy. Soc. Lond. A***240** 599

[26] Leslie-Pelecky D L, Rieke R D 1996 Magnetic Properties of Nanostructured Materials *Chem. Mater.* **8** 1770

[27] Murdock E S, Simmons R F and Davidson R 1992 Roadmap for 10 Gbit/in2 Media: Challenges *IEEE Trans. Magn.* **28** 3078

[28] Mallick A, Mahapatra S, Mitra A and Chakrabarti P K 2016 Soft magnetic property and enhanced microwave absorption of nanoparticles of $Co_{0.5}Zn_{0.5}Fe_2O_4$ incorporated in MWCNT *Journal of Magnetism and Magnetic Materials* **416** 181

[29] Danilyuk A L, Prudnikava A L, Komissarov I V, Yanushkevich K I, Derory A, Normand F L, Labunov V A and Prischepa S L 2014 Interplay between exchange interaction and magnetic anisotropy for iron based nanoparticles in aligned carbon nanotube arrays *Carbon* **68** 337

Table I: Raman and magnetic parameters of MPCVD and TCVD grown MWCNTs, obtained from Raman spectroscopy and magnetic M-H hysteresis loops.

Raman parameters	**MPCVD**			**TCVD**		
D peak position (cm^{-1})	1345			1348		
G peak position (cm^{-1})	1575			1573		
D´ peak position (cm^{-1})	1616			1618		
2D peak position (cm^{-1})	2691			2686		
(I_D/I_G) ratio	0.67			0.75		
L_a (nm) = $(560/E_L^4).(I_D/I_G)^{-1}$	24.78 nm			22.12 nm		
Magnetic parameters						
Temperature	300 K	150 K	2 K	300 K	150 K	2 K
Saturation magnetic moments (Ms) (x 10^{-3}) emu	4.04	4.26	4.29	24.81	28.62	31.45
Magnetic remanence moment (Mr) (x 10^{-3}) emu	0.08	0.15	0.23	9.50	13.73	15.64
Magnetic coercivity (H_c) Oe	40	65	80	500	1570	2900
(Mr/Ms) ratios	0.02	0.04	0.05	0.40	0.48	0.50

Figure captions

Fig. 1: Scanning electron microscopy (upper panel) and transmission scanning electron microscopy (lower panel) images of (a) MPCVD and (b) TCVD grown MWCNTs.

Fig. 2: (a) Comparative X-ray diffraction patterns of MPCVD and TCVD grown MWCNTs. (b) Raman spectroscopy of MPCVD and TCVD grown MWCNTs. (c) Deconvoluted Raman spectra of MPCVD grown MWCNTs. (d) Deconvoluted Raman spectra of TCVD grown MWCNTs.

Fig. 3: (a) Magnetic hysteresis M-H loops within the range ± 5T and (b) Magnified M-H loops within the range ± 175 Oe of MPCVD grown MWCNTs at 300K, 150K and 2K respectively. (c) The temperature dependent field-cool (FC) and zero field cool (ZFC) magnetization within the temperature range 2 K - 350 K at magnetic field of 20 Oe and their remnant (REM), $M_{REM} = M_{FC} - M_{ZFC}$.

Fig. 4: (a) Magnetic hysteresis M-H loops within the range ± 5T and (b) Magnified M-H loops within the range ± 7000 Oe of TCVD grown MWCNTs at 300K, 150K and 2K respectively. (c) The temperature dependent field-cool (FC) and zero field cool (ZFC) magnetization within the temperature range 2 K - 350 K at magnetic field of 20 Oe and their remnant (REM), $M_{REM} = M_{FC} - T_{ZFC}$.

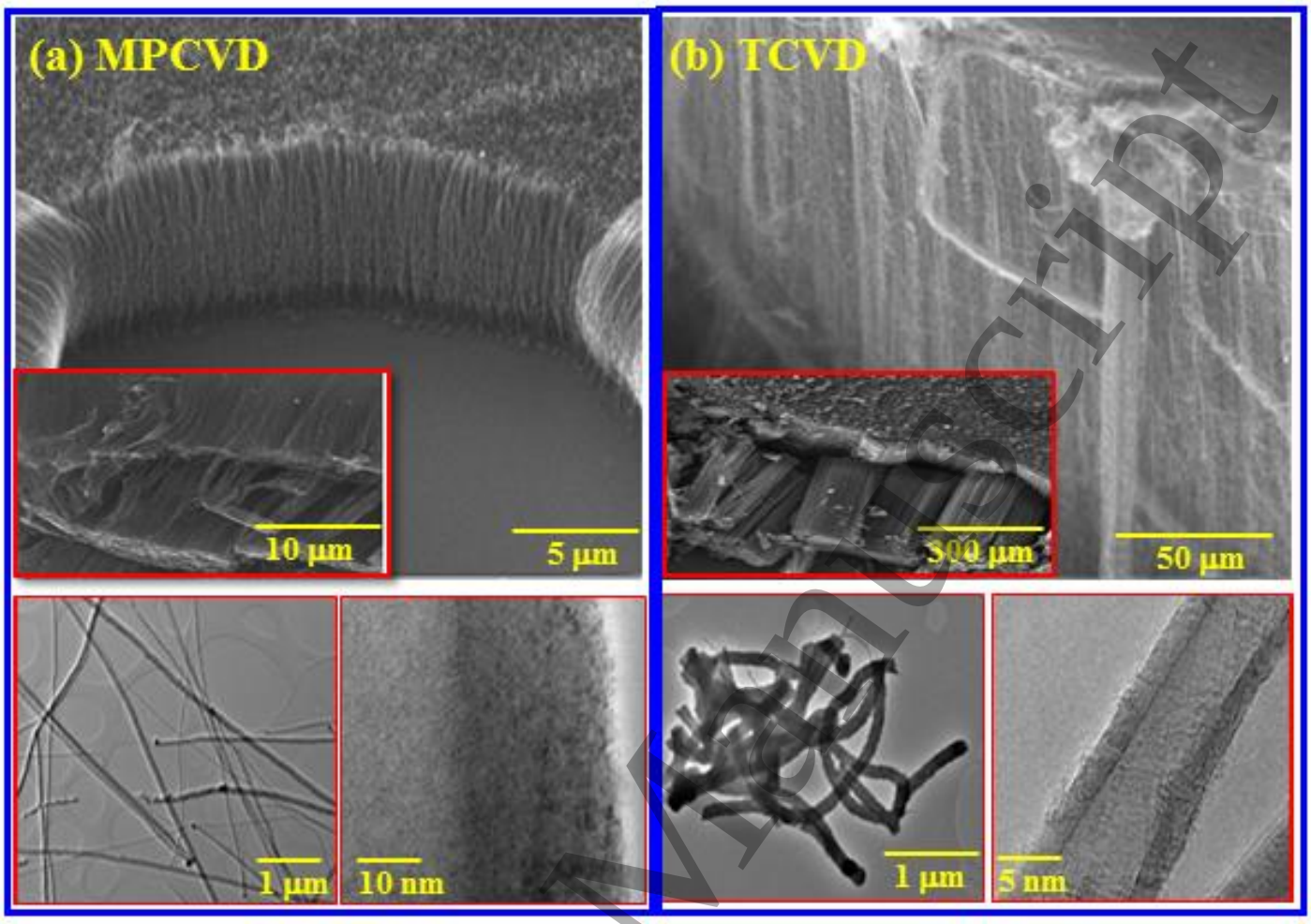

Fig. 1

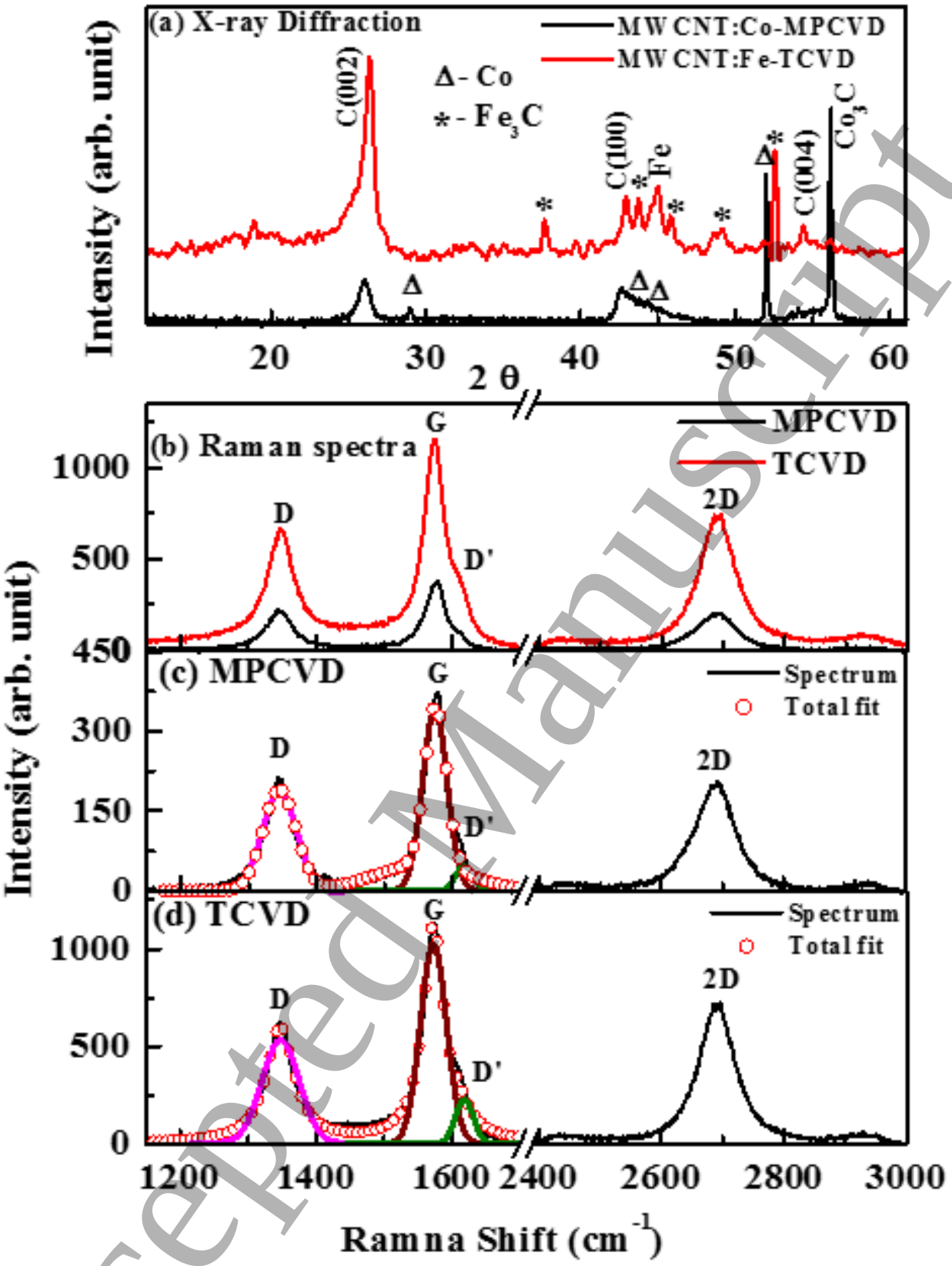

Fig. 2

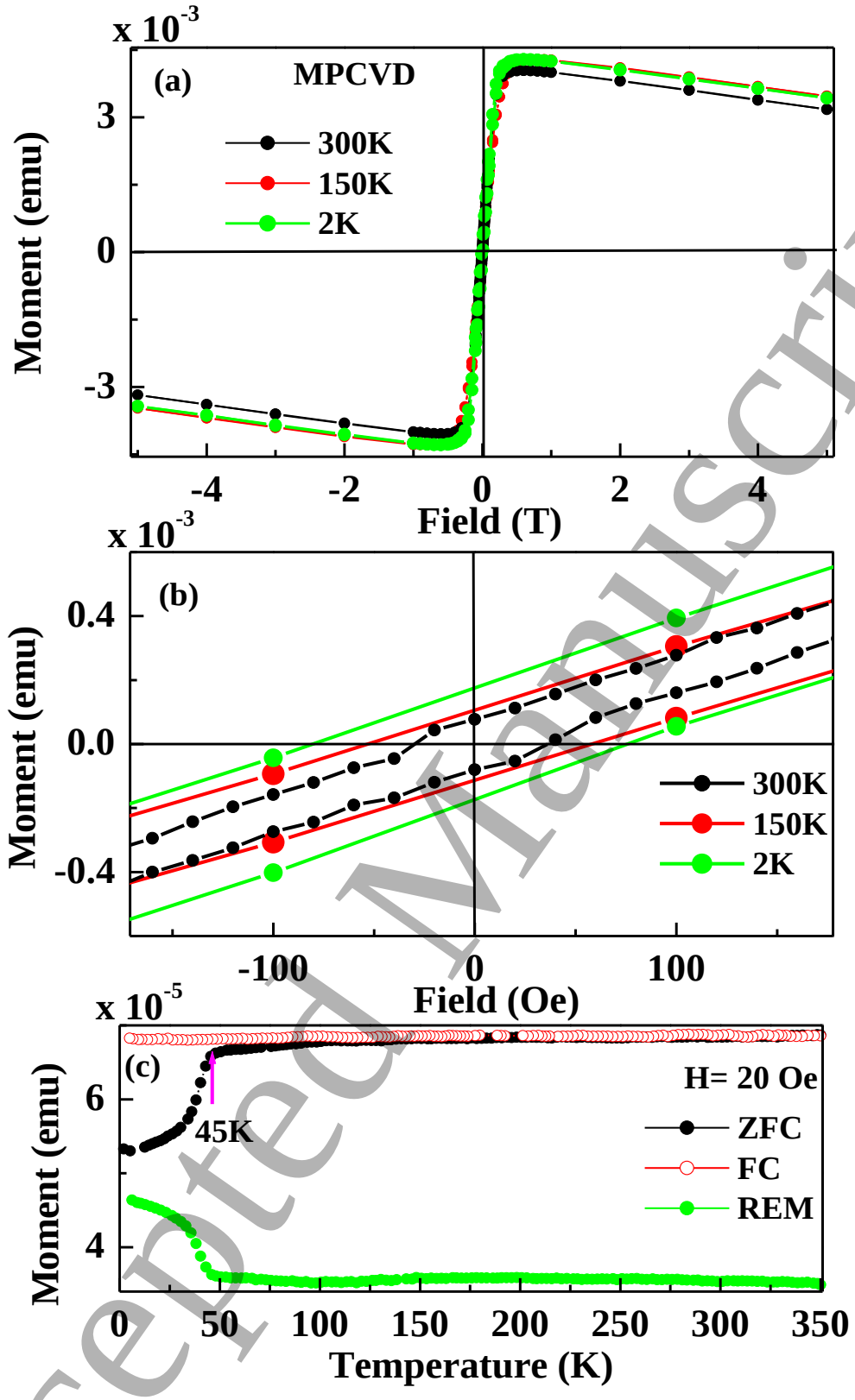

Fig. 3

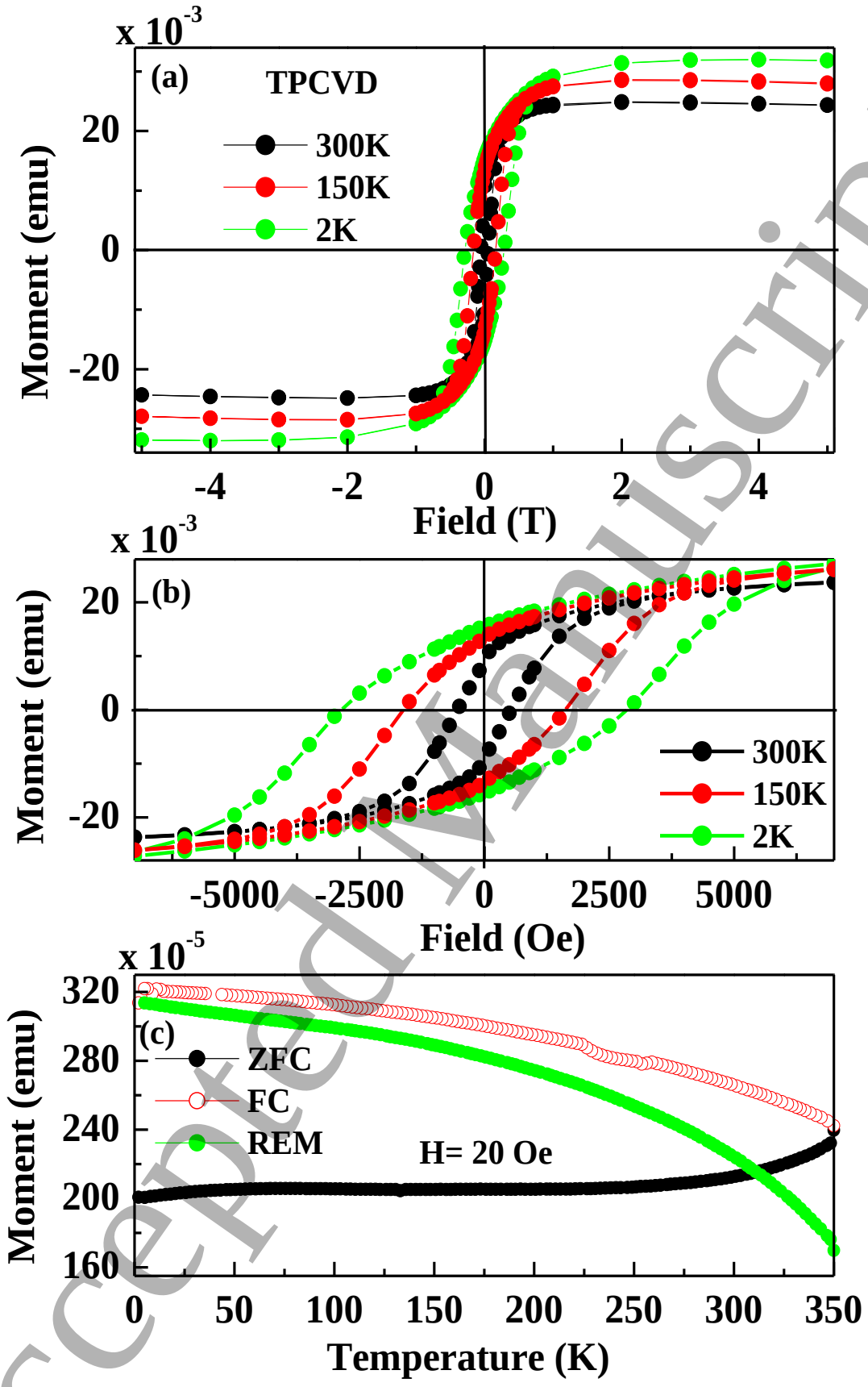

Fig. 4